BIO Integration

Brief Report

Anticancer Efficacy of 5-Fluorouracil-Loaded Chitin Nanohydrogel in Enhanced Skin Cancer Therapy

Yuvraj D. Dange[1,2], Vijay R. Salunkhe[2,*], Sandip M. Honmane[1,*] and Pradnya S. Marale[3]

Abstract

The pyrimidine analog 5-flurouracil (5-FU) is effective against solid tumors. However, the half-life of intravenously administered 5-FU is less than 20 min, and the compound is quickly eliminated and shows systemic toxicity. This study was aimed at developing a nanohydrogel of 5-FU to improve anticancer drug delivery for skin cancer treatment. We prepared 5-FU Chitin nanoparticles (5-FCHNPs) through the ionic gelation technique, and used a 3^2-factorial design approach to optimize the 5-FCHNPs and nanohydrogel formulations. Subsequently, 5-FCHNP particle size, zeta potential, and entrapment efficiency were evaluated. The optimized nanohydrogel formulation was assessed for pH, spreadability, consistency, morphology, and transmission electron microscopy (TEM), scanning electron microscopy (SEM), and *in vitro* cytotoxicity analyses were conducted. The developed nanohydrogel formulation (5-FNH9) showed 68.40% entrapment efficiency, 72.88% drug release, and 1.418% skin penetration. The IC_{50} value of 5-FU was greater than that of 5-FNH9. The developed 5-FNH exhibited enhanced skin penetration and pH-responsive controlled drug release, and therefore has potential in skin cancer treatment.

Keywords

3^2-factorial design, 5-fluorouracil, Chitin, IC_{50}, nanohydrogel, skin cancer.

[1]Department of Pharmaceutics, Annasaheb Dange College of Pharmacy, Ashta 416301, Maharashtra, India

[2]Department of Pharmaceutical Quality Assurance, Rajarambapu College of Pharmacy, Kasegaon 415404, Maharashtra, India

[3]Department of Pharmaceutical Chemistry, Bharati Vidyapeeth College of Pharmacy, Kolhapur 416013, Maharashtra, India

*Correspondence to: Dr. Vijay R. Salunkhe, Department of Pharmaceutical Quality Assurance, Rajarambapu College of Pharmacy, Kasegaon 415404, Maharashtra, India, Tel:+919975146975. Email: vrsalunkhe@rediffmail.com; Dr. Sandip M. Honmane, Department of Pharmaceutics, Annasaheb Dange College of B Pharmacy, Ashta 416301, Maharashtra, India, Tel: +918600392878. E-mail: sandiphonmane@gmail.com

Received: May 9 2025
Revised: June 1 2025
Accepted: June 21 2025
Published Online: July 7 2025

Available at: https://bio-integration.org/

Introduction

Skin cancer, the most prevalent cancer type, is becoming increasingly widespread globally [1]. Melanoma is a potentially lethal cancer affecting melanocytes in the skin. Melanoma develops from abnormally growing melanocytes [2]. Epidemiological research has linked excessive alcohol consumption and UV damage to melanoma risk [3]. Novel treatments that target cancer cells while sparing healthy cells are urgently needed. Local delivery through transdermal and topical administration is recommended owing to its cost-effectiveness and convenience [4]. Because topical medicines exhibit low absorption through the skin, new drug delivery technologies are required. Nanoparticles, hydrogels, and nanohydrogels enhance drug delivery via skin penetration through controlled release, thereby increasing penetration and drug protection. Transdermal drug delivery of 5-FU offers benefits including enhanced solubility, bioavailability, stability, and half-life; targeted distribution; and diminished adverse effects [5, 6]. Chitin (CH) forms polyelectrolyte complexes, and its OH and $NHCOCH_3$ groups facilitate loading of drug molecules [7]. Natural polymers such as CH are biocompatible and biodegradable, and therefore are suitable for wound dressings, medication release, and tissue engineering applications [1, 8]. Nanogels, nanoscale hydrogels, are therefore attractive drug delivery candidates. Hydrogels' cross-linked polymeric network provides biocompatibility through water retention, low-surface tension, and an ECM-like structure [9]. Their features include responses to environmental stimuli, high drug loading, controlled release, favorable permeability and surface area, and adjustable size [9, 10]. The pyrimidine analog 5-FU disrupts thymidylate synthase and therefore is used to treat numerous solid tumor types [6], including brain, colon, pancreas, breast, liver, and gastrointestinal tumors [6]. Although 5-FU has been approved by the US FDA for topical treatment of basal cell carcinoma and other superficial skin lesions, its therapeutic utility is limited by its rapid degradation, systemic toxicity, and poor skin permeation in traditional formulations [6]. Therefore, formulating 5-FU into advanced delivery

systems that achieve enhanced bioavailability and localized action is essential [11]. Despite the individual therapeutic potential of 5-FU and CH-based hydrogels, their integration into a unified nanohydrogel system tailored for topical cancer therapy remains underexplored. Combining the cytotoxic efficiency of 5-FU with the dermal compatibility and functional versatility of CH nanogels provides a novel platform that might potentially overcome the limitations of conventional treatments. In this study, we developed a CH-based nanohydrogel for effective delivery of 5-FU, with aims of enhancing drug stability, controlled release, and skin penetration. To optimize the formulation, we used a 3^2 factorial design enabling systematic evaluation of key formulation factors and their interactions. This statistical approach not only decreased the number of experiments required but also aided in efficient identification of optimal conditions. Our system combining the therapeutic potential of 5-FU with the favorable properties of CH nanogels offers a promising alternative to conventional delivery methods that may decrease systemic adverse effects and improve local treatment outcomes. Beyond skin cancer, this nanohydrogel platform may find broader applications in topical treatments for other dermatological conditions, targeted cancer therapies, and personalized transdermal delivery systems, thus opening avenues to future translational and clinical research.

Materials and methods

Materials

The 5-FU was provided free of charge by Cipla Pharmaceuticals Ltd. in Margao, Goa, India. All other chemicals were of analytical grade.

Preparation of 5-FCHNPs

The 5-FCHNPs were prepared through the ion-gelation technique. Briefly, 100 mL 1% acetic acid was used to dissolve 75, 100, or 125 mg CH. Separately, a 0.1% w/v 5-FU dispersion was generated in phosphate buffer (pH 4.7). The 5-FU solution was slowly added to the CH solution with a microsyringe. Subsequently, 2 mL (0.2 mg/mL) sodium tripolyphosphate (TPP) solution was added, agitated for 10 minutes at 5000, 7500, and 10000 rpm, and allowed to stand at room temperature for 2 hours [12]. Details of the formulation's variable components are shown in **Table 1**.

3^2 Factorial design for 5-FCHNP preparation

The experimental design used a 3^2-factorial approach in Design Expert (Version 13.0, Stat-Ease Inc., USA). The independent variables, stirring speed and CH concentration, influenced the dependent variables, Y1 (particle size), Y2 (zeta potential), and Y3 (entrapment efficiency) (summarized in **Table 1**). ANOVA was used to analyze the factors affecting these responses, and three-dimensional response surface and contour plots were constructed to illustrate the relationships between the factors and the responses [13].

Evaluation of 5-FCHNPs

Particle size and zeta potential

The dynamic light scattering technique (HORIBA Scientific SZ-100) was used to assess the average particle size and surface charge [6].

Percentage drug entrapment

The percentage drug entrapment (PDE) for each formulation was calculated with the centrifugation method [14, 15] and the following formula:

$$\mathrm{PDE} = \frac{\mathrm{A} - \mathrm{B}}{\mathrm{A}} \times 100 \quad (1)$$

Table 1 The 3^2-Factorial Design for 5-FCHNP Preparation

Std.	Run	Factor 1	Factor 2	Response 1	Response 2	Response 3
		Polymer concentration (mg/100 mL) (A)	Stirring speed in (rpm) (B)	Particle size (nm) (Y1)	Zeta potential (mV) (Y2)	% EE (Y3)
3	1	125	5000	565.2	44.5	63.67
9	**2**	**125**	**10000**	**101.3**	**27.3**	**68.4**
6	3	125	7500	344.6	23.3	65.1
8	4	100	10000	121.5	28.81	65.24
2	5	100	5000	545.4	40.1	62.8
5	6	100	7500	318.7	24.9	63.95
4	7	75	7500	316.4	22.1	61.9
1	8	75	5000	479.6	32.8	61.23
7	9	75	10000	168.5	31.2	60.79

EE, entrapment efficiency.
Bold values indicate optimized batch parameters.

Development of 5-FU nanohydrogel

Through a mixing process, optimized 5-FCHNPs (F9) were incorporated into a hydrogel structure. Carbopol 940 was used as a gelling agent to construct a 1% w/w 5-FCHNP gel. The mixture was homogenized for 1 hour at 800 rpm. The pH was adjusted to skin pH by addition of glycerol and triethanolamine.

3^2 factorial design for 5-FU nanohydrogel development

We used a 3^2 factorial design in Design Expert (Version 13.0, Stat-Ease Inc., USA) to optimize independent factors, such as triethanolamine and carbopol concentrations, for nanohydrogel formulation. The analyzed dependent variables comprised viscosity, drug release, and skin penetration (**Table 2**). Correlations and interactions were visualized through 3D contour and response surface plots.

Evaluation of 5-FU nanohydrogel

Physicochemical characterization

The obtained 5-FU nanohydrogel (5-FNH) was visually verified according to phase separation, homogeneity, fluidity, purity, viscosity, pH, spreadability, swelling index, entrapment efficiency, particle size, and zeta potential of gel state [16–19].

FTIR spectroscopy

FTIR spectra were obtained with a Bruker Alpha II FTIR spectrophotometer and captured through a wave number range of 4000–400 cm^{-1}.

Microscopic analysis

The microscopic structures of the synthesized 5-FNH were assessed with a scanning electron microscope (JSM-6360, Jeol Instruments, Japan). Size characterization was performed with TEM (JEM-2100 Plus, JEOL Ltd., Tokyo, Japan) [20].

DSC study

DSC thermograms were recorded at a temperature range of 25–500°C under nitrogen gas purging at a flow rate of 40 mL/min to maintain an inert atmosphere [21].

P-XRD analysis

P-XRD patterns for the samples were recorded in the 10–70°/2θ range, with a copper X-ray target with a wavelength of 1.54 Å [22].

Drug release

A cellulose membrane dialysis bag (12 kD, Sigma, Germany) was filled with 500 µg 5-FNH. The dialysis bag was sealed and submerged in a 100 mL beaker containing 50 mL dissolution medium (PBS, pH 7.4) under agitation with a magnetic stirrer at 100 rpm at a temperature of 37 ± 2°C. At predetermined intervals, 2 mL samples were collected and replaced with an equivalent volume of PBS to maintain sink condition [23]. The aliquots were analyzed with a UV spectrophotometer set to 266 nm to determine drug amounts.

In vitro drug diffusion

Drug diffusion from the nanohydrogel was conducted at the physiological skin pH (7.4) and tumor site pH (4.5–6.5) with a modified Franz diffusion cell. The activated cellulose-acetate membrane was positioned between the donor and recipient plates. The 5-FNH formulation (1 g) was placed into the donor chamber. PBS (30 mL) at pH 5.5 or 7.4 served

Table 2 Evaluation of 5-FCHNP-Loaded 5-FNH

Run	Carbopol w/v X1	Triethanolamine (mL) X2	Viscosity (Cp) Y1	Drug Release (%) Y2	Skin Permeation (%) Y3	P. Size (nm) Y4	EE (%) Y5
1	1.5	0.2	865	63.16	1.201	210.5	60.79
2	1	0.3	724	62.24	1.009	189.2	61.9
3	0.5	0.2	985	59.42	1.119	220.7	62.8
4	0.5	0.3	608	60.24	1.152	201.5	65.9
5	1.5	0.3	679	65.89	1.246	193.6	63.95
6	1	0.2	948	63.89	1.106	189.5	63.4
7	0.5	0.4	715	60.24	1.318	205.6	58.6
8	1	0.4	685	65.39	1.283	198.7	62.7
9	**1.5**	**0.4**	**760**	**72.88**	**1.418**	**195.3**	**68.4**

Bold values indicate optimized batch parameters.

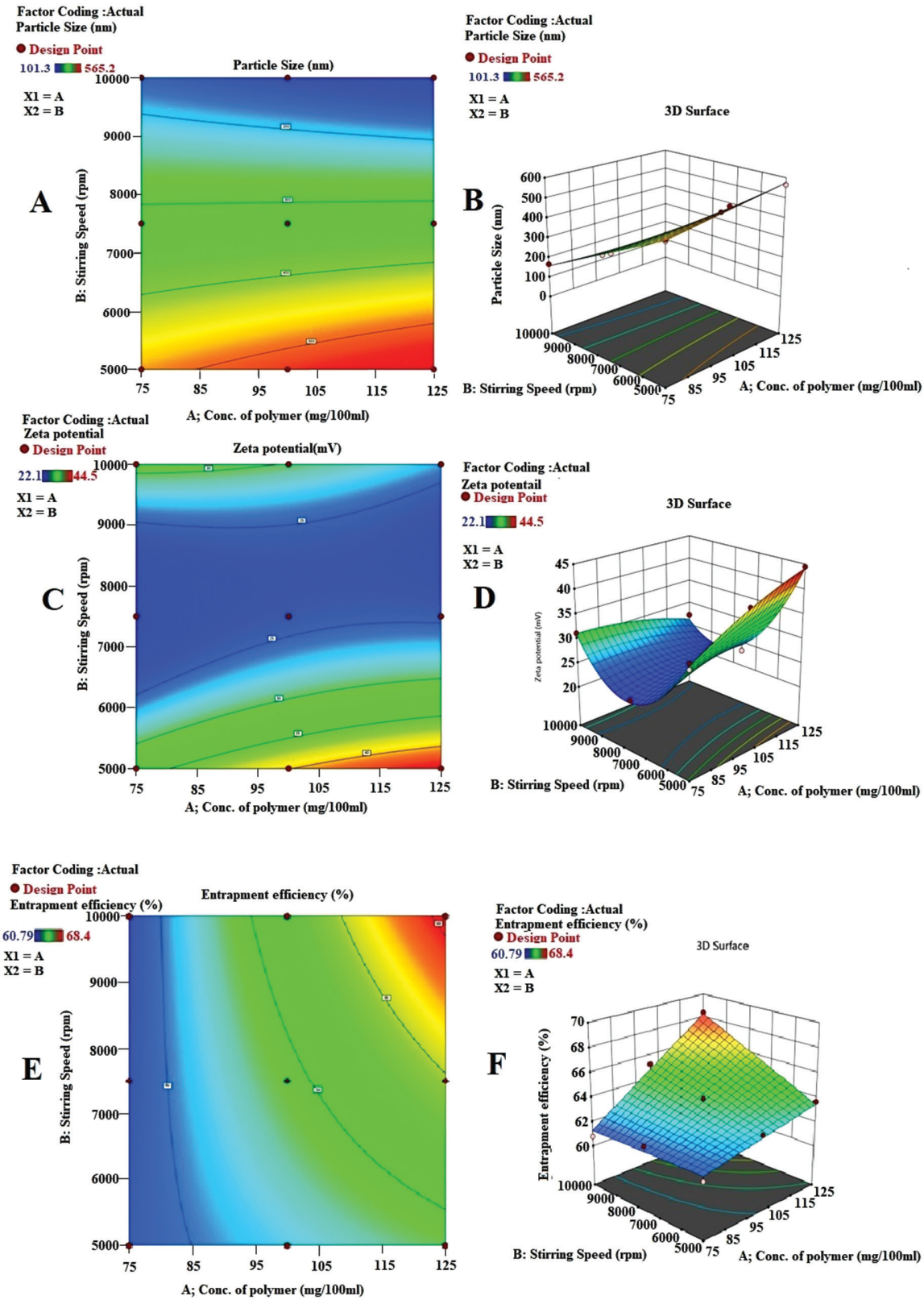

Figure 1 Linear plots (A, C, E) and surface response plots (B, D, F) for particle size, zeta potential, and percentage entrapment efficiency of 5-FCHNPs, respectively.

as the diffusion medium. The system was placed under magnetic stirring (100 rpm) at 37 ± 2°C. The sink condition was maintained by withdrawal of 1 mL sample and replacement with PBS. The 5-FU was determined with a UV-visible spectrophotometer at 266 nm [24, 25].

In vitro cytotoxicity study

The A431 cell line was used to test the cytotoxicity of 5-FNH9 and pure drugs (5-FU) through MTT assays [26]. An ELISA plate reader was used to determine the absorbance

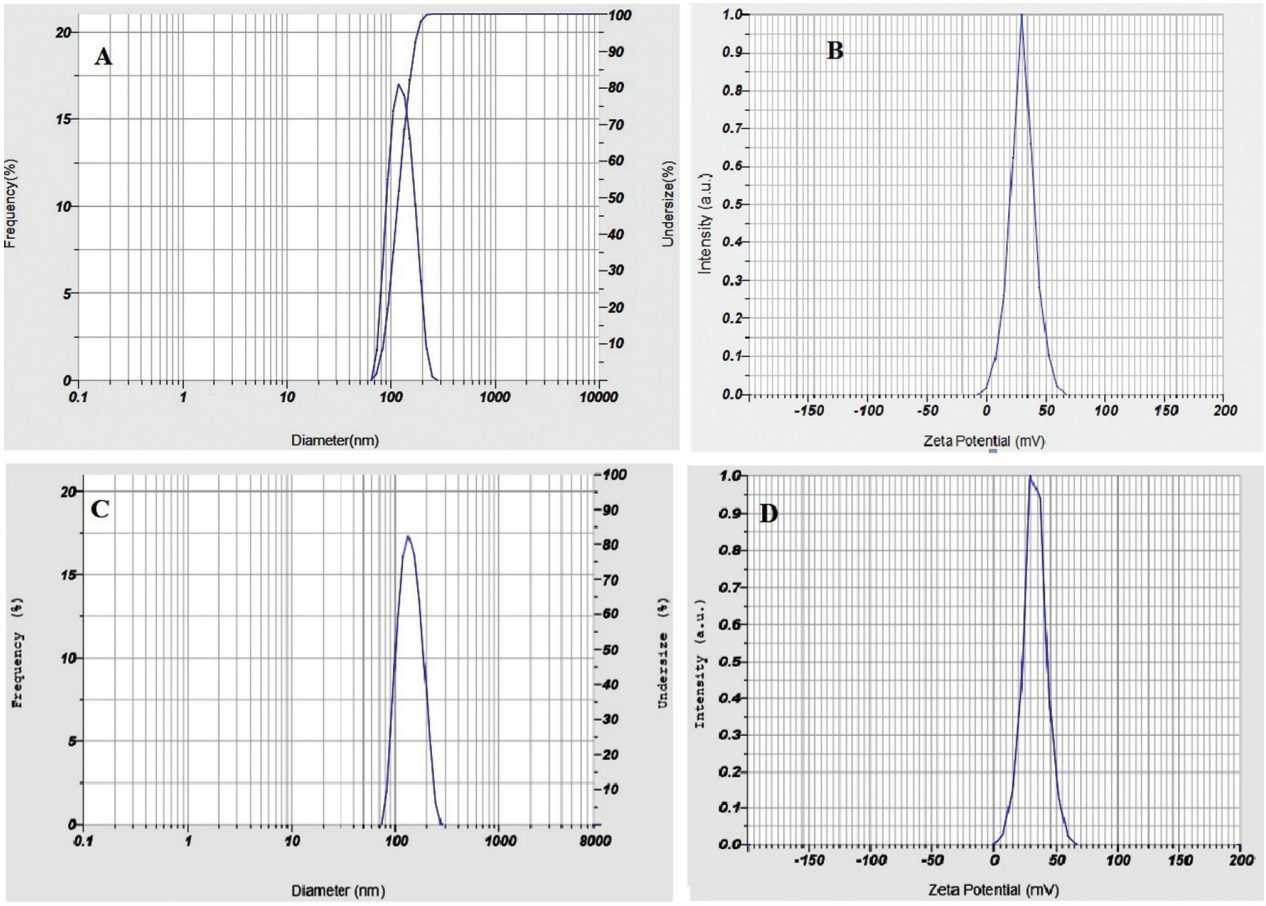

Figure 2 Particle size (A) and zeta potential (B) of optimized nanoparticles (5-FCHNPs9). Particle size (C) and zeta potential (D) of optimized 5-FNH9.

at an optical density of 570 nm. Cell viability was plotted against sample concentration to create a dose-response curve [26]. Equation (2) was used to determine the proportion of viable cells.

$$\% \text{ Cell viability} = \frac{\text{Mean OD of test compound}}{\text{Mean OD of Negative control}} \times 100 \quad (2)$$

where OD is the optical density.

GraphPad Prism version 5.1 was used to determine the IC_{50} value.

Stability study

According to ICH recommendations, an accelerated stability analysis of the nanohydrogel formulation (5-FNH9) was conducted at room temperature (25°C) and a relative humidity of 60% [27].

Results and discussion

Design of experiments (5-FCHNPs)

Particle size

The mean diameters of 5-FCHNPs increased with the CH and TPP concentrations (**Table 1**). The interaction between negatively charged TPP and CH was key for synthesis of 5-FCHNPs. The quadratic model identified the best data patterns, for which the equations fit well. The particle size equation was:

$$Y1 = +329.02 + 7.77A - 199.82B - 38.20AB \quad (3)$$

where Y1 is the particle size, polymer concentration is factor A, and stirring speed is factor B.

Factor A positively influenced Y1, thus indicating that particle size increased with increasing polymer concentration. Factor B negatively affected Y1, thus indicating that particle size decreased with increasing stirring speed (**Figure 1A, B**). This behavior was likely to have arisen from CH and TPP ionic cross-linking, in agreement with similar findings from a prior study [28]. The particle size distribution of the optimal formulation (5-FCHNPs-9) is shown in **Figure 2A**.

Zeta potential

The zeta potential reveals particle charge and dispersion stability; effective stabilization requires a surface charge value within +30 mV and −30 mV [26]. Freshly made 5-FCHNPs showed zeta potentials ranging from 22.1 to 44.5 mV, thereby indicating adequate charge and mobility to avoid aggregation (**Table 1**) [29].

Table 3 Statistical Analysis of the 3^2-Factorial Experimental Design used to Develop the Nanohydrogel

Response	Quadratic Model			
	P Value	R^2	Adjusted R^2	Predicted R^2
Viscosity	0.0050	0.9870	0.9653	0.8682
Percentage drug release	0.0451	0.9419	0.8450	0.3281
Skin permeation	0.0411	0.9455	0.8547	0.5822

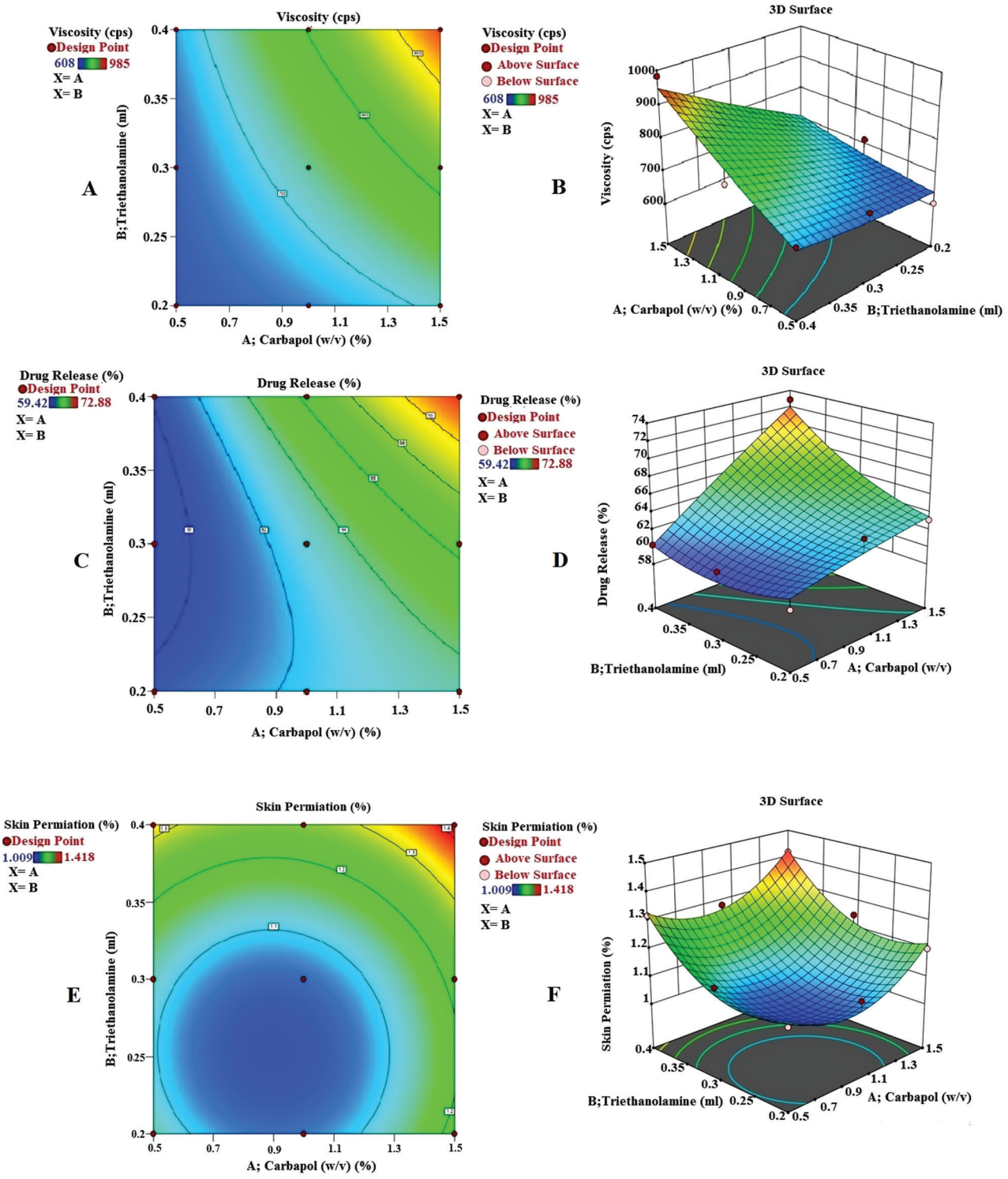

Figure 3 Surface response plots (B, D, F) and linear plots (A, C, E) for investigation of 5-FNH viscosity, percentage drug release, and percentage skin penetration, respectively.

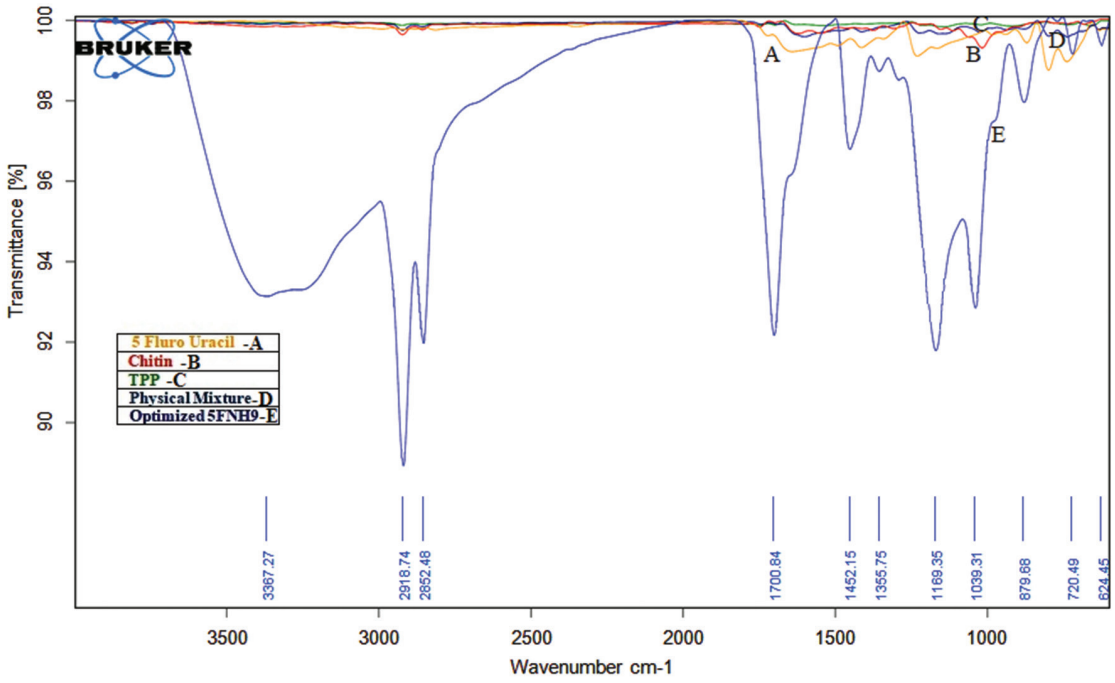

Figure 4 FTIR spectra of 5-FU, physical mixture, and 5-FNH9.

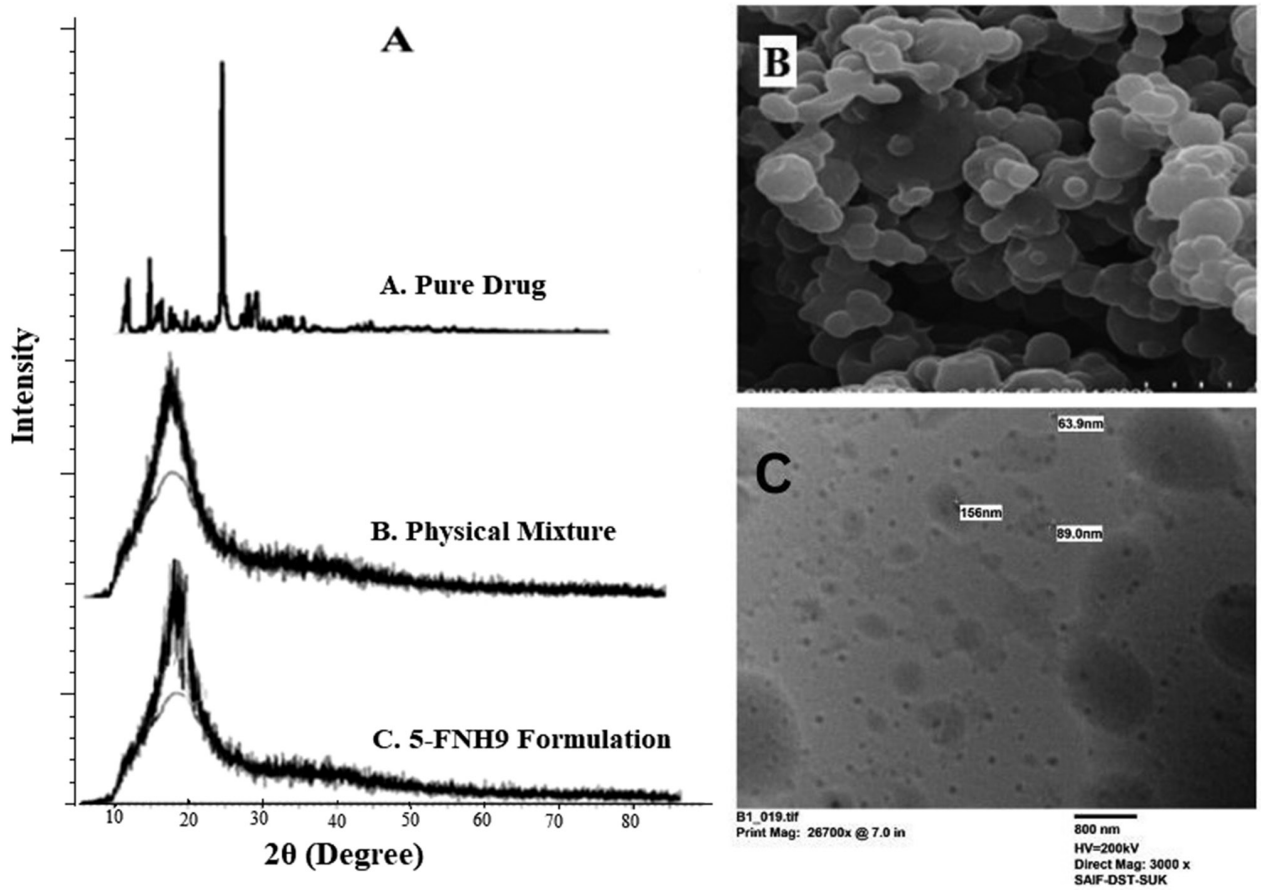

Figure 5 P-XRD of 5-FU, physical mixture, and 5-FNH9 (A), SEM (B), and TEM (C).

The model was represented by the following equation:

$$Y2 = +24.15 + 1.50A - 5.01B - 3.90AB - 1.07A^2 + 10.68B^2 \quad (4)$$

where Y2 is the zeta potential, factor A is the polymer concentration, and factor B is the stirring speed.

The zeta potential increased with increasing polymer concentration but decreased with stirring speed

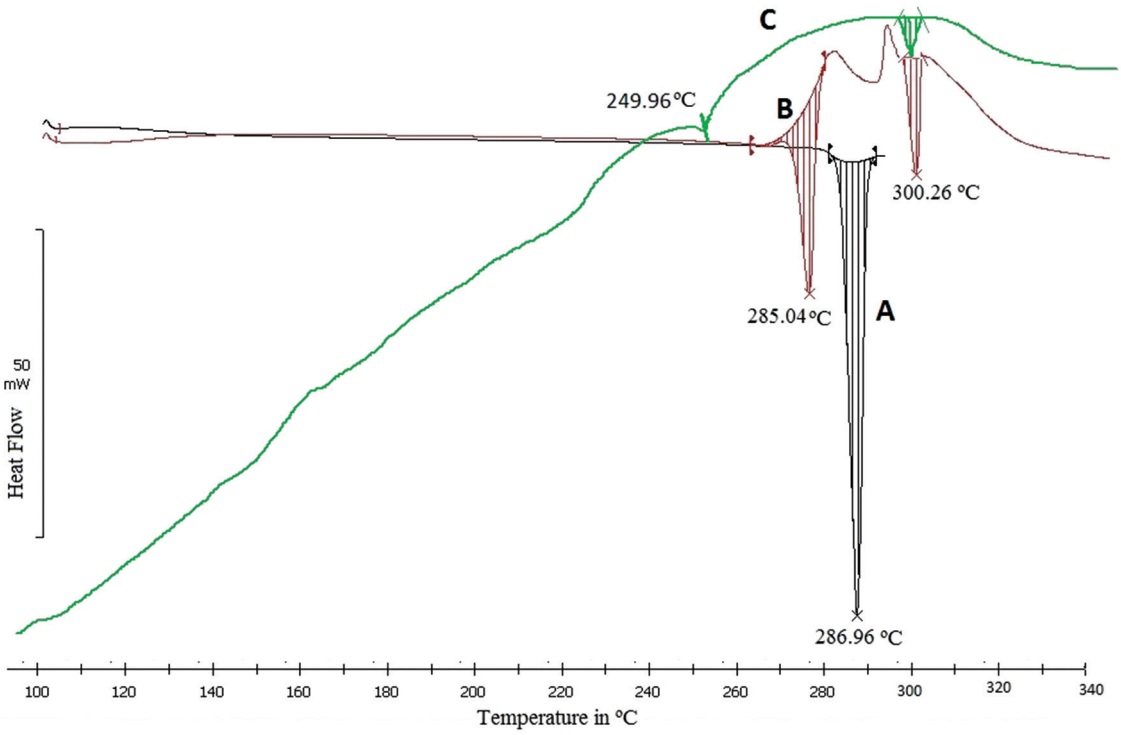

Figure 6 DSC thermogram of pure 5-FU (A), physical mixture (B), and optimized 5-FNH9 (C).

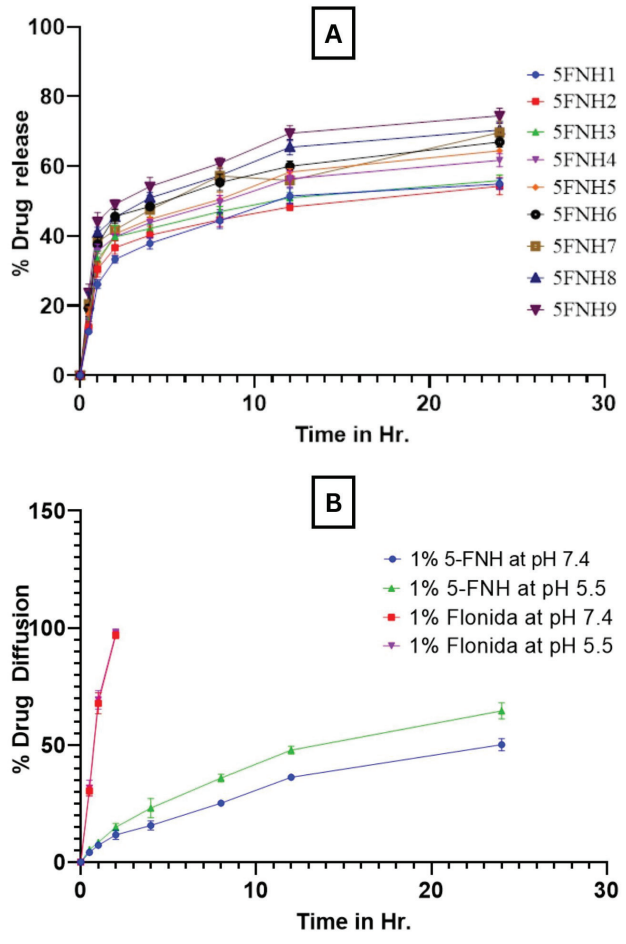

Figure 7 *In vitro* drug release of 5-FNH1 to 5-FNH9 (A), and *in vitro* drug diffusion of 1% 5-FNH9 and 1% Flonida cream (standard marketed formulation) at various pH levels (B).

(**Figure 1C, D**). **Figure 2B** displays the zeta potential of the optimized formulation (5-FCHNPs9).

Entrapment efficiency

The percentage entrapment efficiency for all formulations ranged from 60.79% to 68.40% (**Table 1**). Maximizing the entrapment efficiency while achieving a small particle size is essential for nanoparticle production, because these characteristics substantially influence drug encapsulation. These results were likely to have arisen from ionic cross-linking between TPP and the unbound CH in the dispersion, as demonstrated in previous studies [28, 30]. Entrapment efficiency was positively influenced by both independent factors A and B (**Figure 1E, F**). A mathematical explanation of entrapment efficiency is as follows:

$$Y3 = +63.68 + 2.21\,A + 1.12B + 1.29AB \quad (5)$$

where Y3 is the entrapment efficiency, factor A is the polymer concentration, and factor B is the stirring speed.

Design of experiments (5-FNH)

Our findings suggested that quadratic modeling best explained the data patterns and highlighted the significant influences of triethanolamine (0.2 to 0.4 mL) and carbopol (0.5 to 1.5%) concentrations on the studied phenomena (**Table 3**).

The viscosity (Y1) correlation is described by the following equation:

$$Y1 = +742.33 + 137.67X1 + 40.33X2 + 10.75X1X2 + 62X1^2 - 14X2^2 \quad (6)$$

Table 4 Release Kinetics for the 5-FNH9 Nanohydrogel Formulation

Release Medium	Correlation Coefficient (R^2)				
	Zero-order Kinetics	First-order Kinetics	Higuchi Kinetics	Hixon-Crowell Kinetics	Korsmeyer–Peppas Kinetics
PBS, pH 7.4	**0.998**	0.987	0.955	0.993	0.982
PBS, pH 5.5	**0.997**	0.988	0.969	0.994	0.975

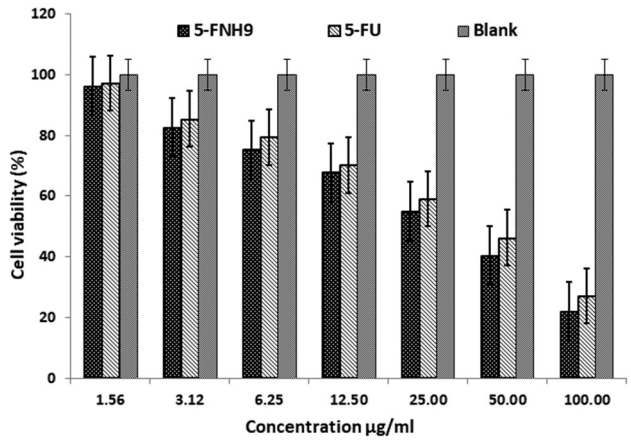

Figure 8 Cytotoxicity studies of pure 5-FU solution, FNH9, and formulation without drug at 48 h toward A431 cells.

This equation indicates that both carbopol (X1) and triethanolamine (X2) positively influence viscosity, which markedly increased with increasing concentrations of polymers and triethanolamine (**Figure 3A and B**) [29].

The drug release (Y2) correlation is described by the following equation:

$$Y2 = +62.92 + 3.67X1 + 2.01X2 + 2.22X1X2 - 0.2017X1^2 + 1.37X2^2 \quad (7)$$

The favorable effects of both carbopol (X1) and triethanolamine (X2) parameters on drug release are shown by the equation (**Figure 3C, D**). The concentrations of triethanolamine and carbopol enhance drug loading and consequently promote drug release [31].

Table 5 IC_{50} Values of Pure 5-FU Solution and 5-FNH9 Formulation (µg/mL) Against A431 Cells After 48-h Incubation

Batch Codes	IC_{50} Value*
Pure 5-FU	54.28 ± 0.23
5-FNH9	47.65 ± 0.15
Blank	746.54 ± 0.22

Mean ± SD is represented by each value, with n = 6.

Skin penetration is increased by the combined effects of A and B, according to the following equation.

$$Y3 = +1.06 + 0.0460X1 + 0.0988X2 + 0.0045X1X2 + 0.1097X1^2 + 0.1052X2^2 \quad (8)$$

Figure 3E and F illustrates effect of concentrations of carbopol (X1) and triethanolamine (X2) on skin penetration. Possible explanations for this activity include enhanced polymer activation in the presence of triethanolamine.

Evaluation of 5-FNH

The developed nanohydrogel's pH decreased from 6.8 to 5.7. A pH range of 6.5–6.8, which is close to the typical pH of human skin, was chosen for the optimized 5-FNH to ensure its safety and suitability for use [23, 25]. The 5-FNH9 formulation was determined to have optimal pH, spreadability, and viscosity with a swelling index of 317 ± 0.72, and therefore was considered the most ideal nanohydrogel formulation (**Table 2**) [23, 26].

The optimal 5-FNH9 had a PDI of 0.301 and a mean vesicle size of 195.3 nm (**Figure 2C**). The surface charge of optimized 5-FNH9 was 29.9 mV, thus demonstrating stability [26]. A positively charged hydrogel might achieve enhanced skin adherence because of interactions with negatively charged skin surface elements [23]. All batches showed entrapment efficiencies of 58.60%–68.40%. The formulation was optimized according to entrapment efficiency and particle size, and the optimized formulation (5-FNH9) achieved 68.40% entrapment efficiency (**Table 2**) [32, 33]. FTIR spectra (**Figure 4**) confirmed successful 5-FU entrapment within CH-TPP NPs, with no drug-excipient interaction indicated by the shift. Similar results have been found in previous investigations [26, 34]. SEM micrographs of optimized 5-FHN9 showed a smooth round shape (**Figure 5B**). A TEM study (**Figure 5C**) indicated diameters of 141–120 nm. Sharp melting endotherms in DSC at 286.96°C were visible in the DSC thermogram of pure 5-FU, thus indicating its crystalline form [34]. The 5-FNH formulation showed slight changes with 5-FU melting endotherms broadening at 249.96°C. Our findings (**Figure 6**) [23, 34] indicated drug entrapment within a

Table 6 Stability Study of Nanohydrogel (5-FNH9)

Days	pH	% EE	Zeta Potential	Viscosity	Appearance
0	6.1 ± 1.10	68.4 ± 0.32	29.9 ± 0.22	985 ± 0.72	+++
30	6.2 ± 0.98	68.1 ± 0.84	29.8 ± 0.14	986 ± 1.15	+++
60	6.4 ± 0.43	67.8 ± 0.72	31.5 ± 0.56	987 ± 2.35	+++
90	6.7 ± 0.10	67.2 ± 0.58	32.16 ± 0.46	987 ± 0.72	+++

polymer matrix with reduction in crystallinity. In the diffractogram of 5-FNH9 (**Figure 5A**), 5-FU showed a strong P-XRD signal indicating crystalline powder. The 5-FNH9 formulation showed few diffusive peaks, indicating amorphous 5-FU [34].

All batches achieved 53.78–72.88% drug release within 24 h. The optimized 5-FNH9 nanohydrogel released 72.88% of the drug over 24 h (**Figure 7A**). Our results therefore indicated that 5-FNH is suitable for transdermal drug delivery. The compound 5-FNH9 exhibited 24.34% and 34.72% drug release at pH 7.4 and pH 5.5, respectively, within 12 h. In contrast, commercial 1% Flonida cream demonstrated faster diffusion, releasing 95.67% of the drug in 4 h (**Figure 7B**). To analyze *in vitro* drug release data, we used mathematical models including Korsmeyer-Peppas, Hixon-Crowell, Higuchi, zero-order, and first-order models. According to the R^2 values (**Table 4**), zero-order kinetics was the best-fit model [23], thus suggesting controlled release.

Cell survival decreased with increasing concentrations of optimized 5-FU nanohydrogel and 5-FU, thus showing dose-dependent cytotoxicity (**Figure 8**). The finding that the 5-FNH9 formulation was more cytotoxic to A431 cells than the pure 5-FU solution at all concentrations further suggested that the formulation without drug was biocompatible and nontoxic, and did not affect cell viability. **Table 5** shows IC_{50} values for the pure 5-FU, 5-FNH9, and the formulation without drug. The pH, zeta potential, viscosity, and appearance of the 5-FNH9 formulation tested at 0-, 30-, 60-, and 90-day intervals were found to be stable (**Table 6**). The entrapment efficiency of 5-FNH9 at 25°C did not substantially differ over 90 days in stability testing (P >0.05) (**Table 6**).

Conclusion

The nanohydrogel exhibited favorable swelling index values and spreadability properties. A zero-order matrix model was shown by *in vitro* drug release kinetics, thus indicating controlled release from the polymer matrices. The 5-FNH formulation showed more drug release at acidic pH 5.5 (tumor site pH) than the normal pH 7.4, thus facilitating targeted delivery to the acidic environment of cancerous cells. *In vitro* cytotoxicity tests revealed that the nanohydrogel formulation (5-FNH9), in contrast to the pure drug, exhibited enhanced 5-FU distribution in A431 cells and high cytotoxicity. The developed 5-FU-loaded CH nanohydrogel has promising potential for topical delivery in the treatment of skin cancer, by enabling pH-responsive controlled release and improved formulation characteristics. However, further *in vivo* studies are required to assess the bioavailability, pharmacokinetics, and pharmacodynamics of the formulation to confirm its therapeutic effectiveness. Although CH is a biodegradable and biocompatible polymer, its *in vivo* safety and compatibility must be thoroughly evaluated. Future work should focus on optimizing these parameters to support clinical translation and the development of an effective targeted anticancer therapy.

Beyond its potential for treating skin cancer, this nanohydrogel platform offers a versatile foundation for broader biomedical applications. Its tunable release profile, biocompatibility, and responsiveness to environmental stimuli are suitable for delivery of a wide range of therapeutic agents, including antibiotics, anti-inflammatory agents, and gene-based therapies. The platform could also be adapted for other skin-associated disorders such as psoriasis, chronic wounds, or fungal infections. Moreover, the incorporation of diagnostic agents might pave the way to theranostic applications combining treatment with real-time monitoring. With further development, this system holds promise for not only oncology but also the advancement of personalized and precision medicine in dermatology and other fields.

Data availability statement

All data generated or analyzed during this study are included in this article. Additional data are available from the corresponding author upon reasonable request.

Ethics statement

No direct interactions with human or animal subjects were involved. Therefore, ethical approval and informed consent were not required.

Author contributions

V.R.S. conceived and designed the study. Y.D.D. performed the experiments and collected the data. S.M.H. analyzed and interpreted the data. Y.D.D., S.M.H., and P.S.M. drafted the manuscript. S.M.H. critically revised the manuscript for intellectual content. All authors read and approved the final manuscript.

Funding

No funding or sponsorship was received for this study.

Acknowledgment

The authors thank the Principal and management of Rajarambapu College of Pharmacy, Kasegaon, Maharashtra, India. The authors also thank the Principal and management of Annasaheb Dange College of B. Pharmacy, Ashta, Maharashtra, India, for providing the facility to complete this research.

Conflict of interest

The authors declare that there are no conflicts of interest.

References

[1] Mangalathillam S, Rejinold NS, Nair A, Lakshmanan VK, Nair SV, et al. Curcumin loaded chitin nanogels for skin cancer treatment via the transdermal route. Nanoscale 2012;4(1):239-50. [PMID: 22080352 DOI: 10.1039/c1nr11271f]

[2] Zheng D, Li X, Xu H, Lu X, Hu Y, et al. Study on docetaxel-loaded nanoparticles with high antitumor efficacy against malignant melanoma. Acta Biochim Biophys Sin 2009;41(7):578-87. [PMID: 19578721 DOI: 10.1093/abbs/gmp045]

[3] Ouhtit A, Ananthaswamy HN. A model for UV-induction of skin cancer. J Biomed Biotechnol 2001;1(1):5-6. [PMID: 12488619 DOI: 10.1155/S1110724301000031]

[4] Singh MD, Mital N, Kaur G. Topical drug delivery systems: a patent review. Expert Opin Ther Pat 2016;26(2):213-28. [PMID: 26651499 DOI: 10.1517/13543776.2016.1131267]

[5] Dange Y, Salunkhe V, Honmane S. Design, development and optimization of 5-fluorouracil nanohydrogel for improved anticancer therapy. BioNanoSci 2024;14:1696-714. [DOI: 10.1007/s12668-024-01315-1]

[6] Kaspar D, Linder J, Zöllner P, Simon U, Smola H. Economic benefit of a polyacrylate-based hydrogel compared to an amorphous hydrogel in wound bed preparation of venous leg ulcers. Chronic Wound Care Manag Res 2015;2015:63-70. [DOI: 10.2147/cwcmr.s78580]

[7] Arunraj TR, Rejinold NS, Kumar NA, Jayakumar R. Doxorubicin-chitin-poly(caprolactone) composite nanogel for drug delivery. Int J Biol Macromol 2013;62:35-43. [PMID: 23973498 DOI: 10.1016/j.ijbiomac.2013.08.013]

[8] Hiranpattanakul P, Jongjitpissamai T, Aungwerojanawit S, Tachaboonyakiat W. Fabrication of a chitin/chitosan hydrocolloid wound dressing and evaluation of its bioactive properties. Res Chem Intermed 2018;44(8):4913-28. [DOI: 10.1007/s11164-018-3344-x]

[9] Sivaram AJ, Rajitha P, Maya S, Jayakumar R, Sabitha M. Nanogels for delivery, imaging and therapy. Wiley Interdiscip Rev Nanomed Nanobiotechnol 2015;7(4):509-33. [PMID: 25581024 DOI: 10.1002/wnan.1328]

[10] Oh JK, Siegwart DJ, Matyjaszewski K. Synthesis and biodegradation of nanogels as delivery carriers for carbohydrate drugs. Biomacromolecules 2007;8(11):3326-31. [PMID: 17894465 DOI: 10.1021/bm070381]

[11] Chen N, Wang H, Ling C, Vermerris W, Wang B, et al. Cellulose-based injectable hydrogel composite for pH-responsive and controllable drug delivery. Carbohydrate Polymer 2019;225:115207. [PMID: 31521293 DOI: 10.1016/j.carbpol.2019.115207]

[12] Li P, Wang Y, Peng Z, She F, Kong L. Development of chitosan nanoparticles as drug delivery system for 5-fluorouracil and leucovorin blends. Carbohydr Polym 2011;85(3):698-704. [DOI: 10.1016/j.carbpol.2011.03.045]

[13] Patil OA, Patil IS, Mane RU, Randive DS, Bhutkar MA, et al. Formulation optimization and evaluation of Cefdinir nanosuspension using 2^3 Factorial design. Marmara Pharm J 2018;22(4):587-98. [DOI: 10.12991/jrp.2018.101]

[14] Honmane SM, Charde MS, Choudhari PB, Jadhav NR. Development and in vitro evaluation of folate conjugated polydopamine modified Carmustine-loaded liposomes for improved anticancer activity. J Drug Deliv Sci Technol 2013;90:105145. [DOI: 10.1016/j.jddst.2023.105145]

[15] Honmane SM, Chimane SM, Bandgar SA, Patil SS. Development and optimization of capecitabine loaded nanoliposomal system for cancer delivery. Indian J Pharm Educ Res 2020;54(2):376-84. [DOI: 10.5530/ijper.54.2.43]

[16] Heping L, Tao Y, Shan L, Long Q, Jingheng N. Preparation and drug-releasing properties of chitosan-based thermo sensitive composite hydrogel. J Korean Chem Soc 2012;56(4):473-7. [DOI: 10.5012/jkcs.2012.56.4.473]

[17] Araujo D, Rodrigues T, Alves VD, Freitas F. Chitin-glucan complex hydrogels: optimization of gel formation and demonstration of drug loading and release ability. Polymers 2022;14(4):785. [PMID: 35215701 DOI: 10.3390/polym14040785]

[18] Bhinge SD, Bhutkar MA, Randive DS, Wadkar GH, Kamble SY, et al. Formulation and evaluation of polyherbal gel containing extracts of *Azadirachtaindica*, *Adhatodavasica*, Piper betle, Ocimumtenuiflorum, and Pongamiapinnata. J Res Pharm 2019;23(01):44-54. [DOI: 10.12991/jrp.2018.107]

[19] Teora SP, Panavaité E, Sun M, Kiffen B, Wilson DA. Hydrogel microparticles as pH-responsive drug carriers for oral administration of 5-FU. Pharmaceutics 2023;15:1380. [PMID: 37242622 DOI: 10.3390/pharmaceutics15051380]

[20] Honmane SM, Charde MS, Osmani RA. Design, development and optimization of carmustine-loaded freeze-dried nano liposomal formulation using 3^2 factorial design approach. Acta Chim Slov 2023;70:204-17. [DOI: 10.17344/acsi.2023.8002]

[21] Honmane S, Hajare A, More H, Osmani RAM, Salunkhe S. Lung delivery of nano liposomal salbutamol sulphate dry powder inhalation for facilitated asthma therapy. Journal of Liposome Res 2018;29(4):332-42. [PMID: 30296863 DOI: 10.1080/08982104.2018.1531022]

[22] Shejawal KP, Randive DS, Bhinge SD, Bhutkar MA, Wadkar GH, et al. Functionalized carbon nanotube for colon-targeted delivery of isolated lycopene in colorectal cancer: in vitro cytotoxicity and in vivo roentgenographic study. J Mate Res 2021;36:4894-907. [DOI: 10.1557/s43578-021-00431-y]

[23] Sahu P, Kashaw SK, Sau S, Kushwah V, Jain S, et al. pH triggered and charge attracted nanogel for simultaneous evaluation of penetration and toxicity against skin cancer: in-vitro and ex-vivo study. Int J Biol Macromol 2019;128:740-51. [PMID: 30699336 DOI: 10.1016/j.ijbiomac.2019.01.147]

[24] Nguyen VC, Nguyen VB, Hsieh MF. Curcumin-loaded chitosan/gelatin composite sponge for wound healing application. Int J Polymer Sci 2013:106570. [DOI: 10.1155/2013/106570]

[25] Thakur RA, Florek CA, Kohn J, Michniak BB. Electrospun nanofibrous polymeric scaffold with targeted drug release profiles for potential application as wound dressing. Int J Pharm 2008;364(1):87-93. [PMID: 18771719 DOI: 10.1016/j.ijpharm.2008.07.033]

[26] Sabitha M, Sanoj Rejinold N, Nair A, Lakshmanan VK, Nair SV, et al. Development and evaluation of 5-fluorouracil loaded chitin nanogels for treatment of skin cancer. Carbohydr Polym 2013;91(1):48-57. [PMID: 23044104 DOI: 10.1016/j.carbpol.2012.07.060]

[27] Ramadon D, Pramesti SS, Anwar E. Formulation, stability test and in vitro penetration study of transethosomal gel containing green tea (Camellia sinensis L. Kuntze) leaves extract. Int J App Pharm 2017;9(5):91-6. [DOI: 10.22159/ijap.2017v9i5.20073]

[28] Jana S, Manna S, Nayak AK, Sen KK, Basu SK. Carbopol gel containing chitosan-egg albumin nanoparticles for transdermal aceclofenac delivery. Colloids Surf B Biointerfaces 2013;114:36-44. [PMID: 24161504 DOI: 10.1016/j.colsurfb.2013.09.045]

[29] Amasya G, Inal O, Sengel-Turk CT. SLN enriched hydrogels for dermal application: full factorial design study to estimate the relationship between composition and mechanical properties. Chem Phys Lipids 2020;228(1):104889. [PMID: 32044298 DOI: 10.1016/j.chemphyslip.2020.104889]

[30] Al-Kassas R, Wen J, Cheng AE, Kim AM, Liu SSM, et al. Transdermal delivery of propranolol hydrochloride through chitosan nanoparticles dispersed in mucoadhesive gel. Carbohydr Polym 2016;153:176-86. [PMID: 27561485 DOI: 10.1016/j.carbpol.2016.06.096]

[31] Chakraborty T, Verma R, Sharma J, Sharma P. 3^2 Full factorial design for optimization of clindamycin phosphate loaded nanogel: a design of experiments (DOE) approach. Int J Pharm Pharm Res 2022;24(4):160-71.

[32] Arica B, Calis S, Kas H, Sargon M, Hincal A. 5-fluorouracil encapsulated alginate beads for the treatment of breast cancer. Int J Pharm 2022;242(1-2):267-9. [PMID: 12176261 DOI: 10.1016/s0378-5173(02)00172-2]

[33] Blanco MD, Guerrero S, Benito M, Fernández A, Teijón C, et al. In vitro and in vivo evaluation of a folate-targeted copolymeric submicro hydrogel based on N-isopropyl acrylamide as 5-fluorouracil delivery system. Polymers 2011;3(3):1107-25. [DOI: 10.3390/polym3031107]

[34] Mohammed AM, Osman SK, Saleh KI, Samy AM. In vitro release of 5-fluorouracil and methotrexate from different thermosensitive chitosan hydrogel systems. AAPS PharmSciTech 2020;21(4):131. [PMID: 32405869 DOI: 10.1208/s12249-020-01672-6]